

Cyanovirin-N binding to Man α 1–2Man functionalized dendrimers†Shane L. Mangold,^a Joel R. Morgan,^a Gregory C. Strohmeyer,^a Angela M. Gronenborn^b and Mary J. Cloninger^{*a}^a Department of Chemistry and Biochemistry and Center for Bioinspired Nanomaterials, 108 Gaines Hall, Montana State University, Bozeman, MT, 59717, USA.

E-mail: mcloninger@chemistry.montana.edu; Fax: 406 994 5407; Tel: 406 994 3051

^b Laboratory of Chemical Physics, National Institute of Diabetes and Digestive and Kidney Diseases, National Institutes of Health, Bethesda, MD, 20892

Received (Pittsburgh, PA, USA) 30th November 2004, Accepted 4th May 2005

First published as an Advance Article on the web 24th May 2005

Man α 1–2Man functionalized G(3) and G(4)–PAMAM dendrimers have been synthesized and characterized by MALDI-TOF MS and NMR spectroscopy. Precipitation assays to assess the binding of the dimannose-functionalized dendrimers to Cyanovirin-N, a HIV-inactivating protein that blocks virus-to-cell fusion through high mannose mediated interactions, are presented.

Introduction

The HIV envelope proteins gp120 and gp41 are heavily glycosylated,¹ containing a preponderance of N-linked high-mannose oligosaccharides.² These are the target for the HIV-inactivating protein Cyanovirin-N (CV-N), an 11 kDa protein that potently interferes with viral entry by binding to Man-8 and Man-9 on gp120.³ The three dimensional structure of CV-N was solved by NMR and X-ray crystallography, and the basis for high-mannose-mediated binding of CV-N was investigated.⁴ It is now generally accepted that both sugar binding sites of CV-N recognize the Man α 1–2Man disaccharide that is present on the terminal branches of the higher oligomannose structures including Man8D1D3 and Man9. Different association constants for dimannoses, trimannoses and other higher mannose oligosaccharides for the two symmetry related carbohydrate binding sites on CV-N revealed slight preferences for one or the other site.⁵ As such, multisite and multivalent protein-carbohydrate interactions are responsible for the unusually tight association between CV-N and the high mannose oligosaccharides. The resulting cross-linking between the protein and the dimannose units at the tips of the complex sugars appear to be pivotal for CV-N's remarkable virucidal activity.⁵

Protein-carbohydrate interactions play critical roles in many biological recognition events,^{6,7} and elucidating the underlying structural basis is a pre-requisite for developing therapeutic agents exploiting this interaction. Carbohydrates are often grafted onto macromolecules in order to study such interactions,⁸ with dendrimers being particularly useful scaffolds for display.^{9,10}

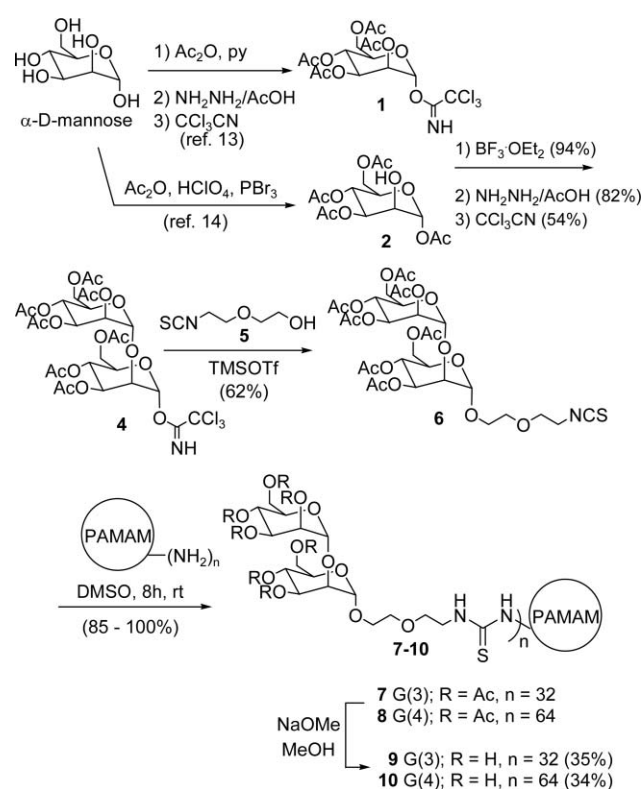
Dendrimers are macromolecular compounds that consist of a series of branches around an inner core,¹¹ and their use as frameworks and as carrier systems for investigating and modulating biological processes is gaining popularity.¹² They are attractive for this type of work because of their size (nanometer scale), their ease of preparation and functionalization, and their ability to display multiple copies of the molecule of interest on their surface for probing biological recognition processes.

To investigate the multivalent binding to CV-N, we functionalized G(3) and G(4)–PAMAM dendrimers with Man α 1–2Man dimannose and used a precipitation assay to quantify the stoichiometry of the CV-N–dendrimer complex. The results

from the precipitation assay are evaluated and compared to those obtained for Concanavalin A (Con A, a multivalent mannose-binding lectin).

Results and discussion

The general procedure for the dimannose functionalization of PAMAM dendrimers is shown in Scheme 1. Following a literature procedure, peracetylation of D-mannose followed by selective deprotection and activation at the anomeric position afforded trichloroacetimidate **1** (53%, 3 steps).¹³ BF₃·OEt₂-mediated coupling of this acceptor with **2**¹⁴ led to the fully acetylated mannoside **3** (94%, not shown).¹⁵ Anomeric deacetylation with hydrazine acetate and reaction with trichloroacetimidate



Scheme 1 Synthesis of dimannose dendrimers.

† Electronic supplementary information (ESI) available: spectral data. See <http://www.rsc.org/suppdata/ob/b4/b417789d/>

gave **4** (44%, 2 steps).¹⁵ Coupling of **4** with the isothiocyanato alcohol **5**^{9a} using TMSOTf yielded the requisite dimannose **6** (62%). We chose to use **5** as the tether between the dimannose and the dendrimer because of **5**'s water solubility (compared to aromatic linkers) and because of **5**'s ease of synthesis and good stability.^{9a} Addition of **6** to the dendrimer followed by global deacetylation resulted in dendrimers **9** and **10**. Dialysis afforded **9** and **10** in purified form.

The ¹H NMR (500 MHz) spectra of acetyl-protected dimannose-functionalized dendrimers **7** and **8** were obtained in d₆-DMSO. The amide protons from the interior of the dendrimer and the thiourea NH resonate the farthest downfield. Signals from the acetyl groups and sugar moieties are observed at 2.0 and 5.0–5.2 ppm, respectively. The complicated pattern of peaks from 2.0 to 4.0 ppm arises from PAMAM protons and additional protons from **6**. Although the ¹H NMR spectra of **9** and **10** are complicated by significant exchange broadening, the absence of peaks at around 2.0 ppm clearly demonstrates that the acetyl groups have been removed (Figures S1 through S4, refer to the supplementary information).

The MALDI-TOF MS of dimannose functionalized dendrimers **7** and **8** are displayed in Fig. 1. For clarity, a smoothing function has been applied to the spectra in Fig. 1; original data are provided in the supporting information (Figures S5 and S6, refer to the supplementary information). The degree of functionalization was determined by subtracting the molecular weight of the PAMAM starting material from the molecular weights of dimannose dendrimers followed by division by 766 (the molecular weight of **6**). Since the experimentally determined M_w of **7** was 27100 g mol⁻¹, subtraction of the molecular weight of the unfunctionalized G3 (6910 g mol⁻¹) and division by 766 suggests that, on average, 26 dimannose groups are present on **7**. The experimentally determined M_w of **8** was 50400 g mol⁻¹, and the equivalent calculation (subtraction of 13500 g mol⁻¹ and division by 766) yields an average 48 dimannose groups on **8**.¹⁶

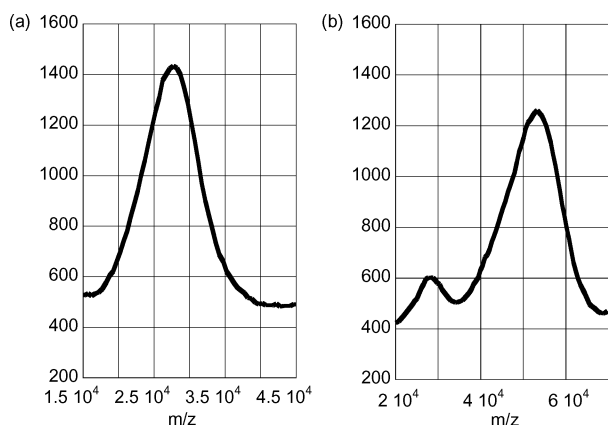


Fig. 1 (a) MALDI spectrum of **7**, (b) MALDI spectrum of **8**.

To evaluate the stoichiometry of the dimannose dendrimer–CV-N interaction, precipitation assays were performed.¹⁷ Serial dilutions of dendrimers **9** and **10** were incubated with a constant concentration of CV-N. At high concentrations of dendrimers (above 43 μM), the Man_α1–2Man functionalized dendrimers induced precipitation of CV-N–dendrimer aggregates. By measuring the absorbance (A₂₈₀) of the supernatant, the quantity of un-precipitated protein was determined. Subtracting the initial concentration of protein from the amount of unprecipitated protein allowed us to determine the amount of protein precipitated as a function of dendrimer concentration. From this, the ratio of CV-N concentration to dendrimer concentration, or the stoichiometry of the complex, was obtained.

The results of the precipitation assays for **9** and **10** are displayed in Fig. 2a. Titration of CV-N with increasing amounts

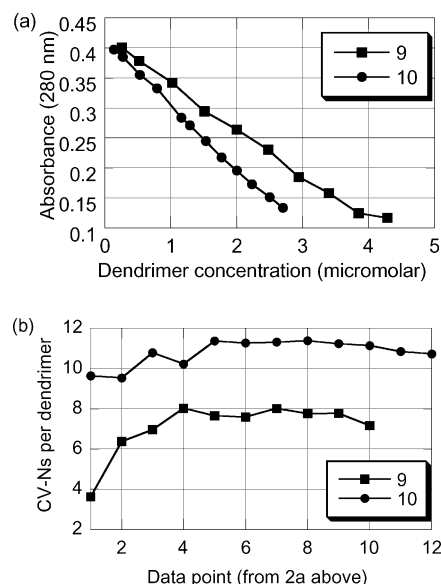
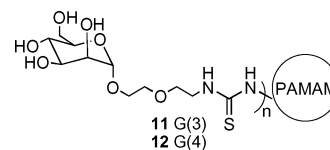


Fig. 2 (a) Absorbance readings (A₂₈₀) from the precipitation assay, (b) Stoichiometry of CV-N–dendrimer interactions.

of dendrimer showed a linear decrease in the absorbance, *i.e.*, the increase in total amount of protein precipitated. For **9**, a constant slope was observed for concentrations up to 4 μM of dendrimer, above which a levelling off occurred. For **10**, a linear decrease was observed for all concentrations of **10** that were evaluated. These data translate to apparent stoichiometries of 8 : 1 and 11 : 1 for CV-N : dendrimer for **9** and **10**, respectively (Fig. 2b).

To determine the maximum number of CV-N proteins that can fit around the Man_α1–2Man functionalized dendrimers **9** and **10**, clay models were constructed based upon the dimensions of the CV-N protein and dendrimers. The CV-N proteins were modelled as ellipsoids with 25 and 55 Å diameters for the short and long axes, respectively (clay models with 1 Å = 1 nm were constructed). The dendrimers were modelled as spheres with diameters of 65 Å for **9** and 83 Å for **10**; these values are reasonable approximations based on previously determined radii of similar dendrimers.^{9a} Optimal packing density suggests that approximately 13 CV-N proteins can fit around **9** and 15 proteins can surround **10**. These theoretical values are significantly higher (4–5 proteins) than the experimentally determined values obtained in the precipitation assays.



The differences between the expected and observed protein : dendrimer ratios are in stark contrast to our previous results with mannose-functionalized dendrimers binding to Concanavalin A (Con A), where a maximum number of sterically allowed proteins was always bound by the dendrimers (Table 1 and Fig. 3b).^{9a} The association constant for binding of mannose

Table 1 Protein : dendrimer ratios for CV-N and Con A^a

Protein	Observed ratio of protein : dendrimer	Theoretical ratio of protein : dendrimer
9	CV-N 8 : 1	13 : 1
10	CV-N 11 : 1	15 : 1
11	Con A 10–11 : 1	9–10 : 1
12	Con A 11–12 : 1	12–13 : 1

^a Con A values are taken from reference 9a.

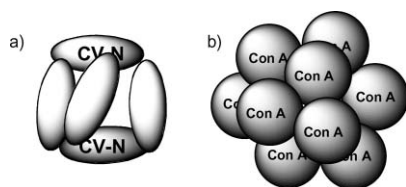


Fig. 3 Schematic representation of (a) unoptimized dendrimer coverage by CV-N and (b) complete dendrimer coating by Con A.

to each Con A binding site is relatively low ($K_a = 9.9 (\pm 0.3) \times 10^3 \text{ M}^{-1}$),¹⁸ while the affinity of CV-N for oligomannose structures is significantly higher (both K_{ds} for CV-N with dimannose are in the micromolar range, two and three orders of magnitude tighter than the binding constant of mannose binding to Con A). Perhaps the binding mechanism for CV-N is governed predominantly by the associative or dissociative rate constant rather than by theoretical maximum occupancy (as with Con A). The substantially higher affinity of CV-N for oligomannose structures may not allow efficient dissociation of CV-N, precluding optimized surface coverage. This effect may be potentiated by the presence of two mannose binding sites on a single protein. It takes only a small number of proteins binding to the dendrimer surface in a non-idealized packing arrangement to enforce a sub-optimal protein coverage (Fig. 3a), easily accounting for the fact that only 60–70% of the total possible number of CV-Ns are bound by **9** and **10**. Clearly, the low number of CV-Ns bound by **9** and **10** is not a function of the available number of dimannose units. Assuming that two dimannose residues are bound by each CV-N, only 62 and 46% of the total dimannose groups are bound by CV-N on **9** and **10**, respectively.

Conclusion

Dimannose functionalized G(3) and G(4) PAMAM dendrimers having on average 26 and 48 dimannose groups per dendrimer were synthesized and characterized. These dendrimers are competent for the recruitment of CV-N. Compared to previously-reported clustering events for mannose functionalized dendrimers with Con A, for which the degree of clustering is limited to a theoretical maximum based on steric considerations, the number of clustered proteins is reduced. The higher association constant of CV-N for dimannose and the specific disposition of two binding sites on a single protein molecule provide one possible explanation for the observed differences between CV-N and Con A recruitment by dendrimers. Although it is counter-intuitive, the degree of lectin clustering on cell surfaces may be attenuated by changes in binding on/off rates, where higher affinities cause lower numbers of proteins to be bound. This finding has important implications for the design of therapeutic agents designed to target multivalent protein–carbohydrate interactions.

Experimental section

General protocols

General reagents were purchased from Aldrich, Sigma, and Acros. PAMAM dendrimers were purchased from Dendritech as aqueous solutions. All MALDI-TOF reference standards were purchased from Sigma. Compounds **1**,¹³ **2**,¹⁴ **4**,¹⁵ and **5**,^{9a} were synthesized as previously reported.

1,3,4,6-Tetra-O-acetyl-2-O-(2,3,4,6-tetra-O-acetyl- α -D-mannopyranosyl)- α -D-mannopyranose (3). The 2,3,4,6-tetra-O-acetyl- α -D-mannopyranosyl trichloroacetimidate **1** (2.76 g, 5.7 mmol) was dissolved in 10 mL of CH_2Cl_2 and combined with 1,3,4,6-tetra-O-acetyl- α -D-mannopyranoside **2** (2.0 g, 5.7 mmol) in 10 mL of CH_2Cl_2 with 4 Å molecular sieves. The solution was cooled to -50°C under N_2 . $\text{BF}_3 \cdot \text{Et}_2\text{O}$ (866 μg ,

6 μmol) was added to the flask, and the solution was allowed to warm to room temperature. The reaction was stirred overnight for 18 h and quenched with 1.5 g of sodium bicarbonate. The reaction mixture was filtered over Celite, concentrated *in vacuo*, and purified by silica gel chromatography (70 : 30 ethyl acetate : hexanes) to yield 3.6 g of white fluffy solid product (94% yield). $^1\text{H NMR}$ (300 MHz, CDCl_3) δ 5.77 (s, 1H), 5.44–5.52 (m, 1H), 5.19–5.43 (m, 4H), 5.02–5.19 (m, 2H), 4.99 (s, 1H), 4.37–4.45 (m, 1H), 4.00–4.47 (m, 7H), 3.74–3.81 (m, 1H), 2.14 (s, 5H), 2.11 (s, 2H), 2.07–2.08 (m, 5H), 2.02 (bs, 5H), 2.00 (s, 3H) ppm. Characterization data matched previously reported values.¹⁵

1-O-(5-isothiocyanato-3-oxapentyl)-3,4,6-tri-O-acetyl-2-O-(2,3,4,6-tetra-O-acetyl- α -D-mannopyranosyl)- α -D-mannopyranose (6). A solution of **4** (633 mg, 810 μmol) and 2-(2-isothiocyanatoethoxy)ethanol (**5**)^{9a} (418 mg, 2.8 mmol) in CH_2Cl_2 was added to 4 Å molecular sieves and cooled to -50°C under Ar (g). After stirring for 1 h, trimethylsilyl trifluoromethane sulfonate (140 μL , 172 mg, 775 μmol) was added and the reaction was allowed to warm to room temperature over 4 h. Benzene (12 mL) and pyridine (7.5 mL) were added, the solution was filtered through celite, and solvents removed *in vacuo*. The product was purified on silica gel (95 : 5 ethyl acetate : hexanes) and recrystallized (3 : 1 ether : petroleum ether) to afford 386 mg of **6** as a white solid (504 μmol , 62% yield). Mp $67\text{--}68^\circ\text{C}$; $^1\text{H NMR}$ (500 MHz, CDCl_3) δ 5.18–5.35 (m, 5H), 4.93 (s, 1H), 4.87 (s, 1H), 4.01–4.19 (m, 6H), 3.92 (m, 1H), 3.79 (m, 1H), 3.58–3.64 (m, 7H), 2.08 (s, 3H), 2.07 (s, 3H), 2.02 (s, 3H), 2.01 (s, 3H), 1.97 (s, 3H), 1.97 (s, 3H), 1.94 (s, 3H) ppm; $^{13}\text{C NMR}$ (125 MHz, CDCl_3 , not observed/overlapped: 1 CH_3CO , 4 CH_3CO) δ 170.8, 170.4, 170.3, 169.8, 169.7, 169.3, 133.1, 99.1, 98.3, 77.0, 70.2, 70.0, 69.7, 69.4, 69.1, 68.5, 68.4, 67.3, 66.4, 66.1, 62.5, 62.1, 45.3, 20.8, 20.7, 20.6 ppm; IR (KBr) 1365, 1737, 2109, 3044; HRMS: calc for $(\text{M} + \text{Na})^+$ $\text{C}_{31}\text{H}_{43}\text{O}_{19}\text{NSNa}$ 788.2048, found 788.2031.

Peracetylated dimannose functionalized G(3)–PAMAM 7. A solution of **6** (35 mg, 46 μmol) in 1 mL DMSO was added to G(3)–PAMAM (6.3 mg, 0.91 μmol) and the solution was stirred for 48 h. Dialysis against DMSO ($\text{MWCO } 3500 \text{ g mol}^{-1}$) and lyophilization afforded 30 mg of pale yellow oily solid **7** (121% yield, some DMSO still present). $^1\text{H NMR}$ (500 MHz, CD_3SOCD_3) δ 7.96 (bs, 1H, amide NH), 7.75 (bs, 1H, amide NH), 7.47 (bs, 2H, $\text{CH}_2\text{NHC}(\text{S})\text{NHCH}_2$), 5.06–5.20 (m, 7H), 4.98 (bs, 1H), 3.99–4.09 (m, 7H), 3.87–3.89 (m, 1H), 3.73–3.79 (m, 2H), 3.58–3.62 (m, 5H), 3.48 (bs, 5H), 3.38 (m, 2H), 3.29 (bs, 2H), 3.13 (bs, 3H), 3.05 (bs, 2H), 2.54–2.70 (m, 4H), 2.47 (s, 2H), 2.33–2.45 (m, 3H), 2.16 (bs, 4H), 2.08 (s, 4H), 2.00 (s, 3H), 1.98 (s, 7H), 1.95 (s, 7H), 1.92 (s, 4H) ppm; $^{13}\text{C NMR}$ (125 MHz, CD_3SOCD_3 , not observed/overlapped: CS, amide CO, CH_3CO , 3 CH_3CO , 2 mannose CO, 5 CH_2N) δ 170.5, 170.4, 170.2, 170.0, 169.9, 169.7, 98.5, 97.9, 76.3, 69.9, 69.5, 69.2, 68.9, 68.5, 68.3, 67.2, 66.0, 62.5, 62.0, 50.0, 33.7, 21.0, 20.9, 20.8, 20.7 ppm; MALDI-TOF MS (pos) 27,100 g mol^{-1} (theoretical MS $\text{C}_{1296}\text{H}_{1988}\text{N}_{154}\text{O}_{668}\text{S}_{32}$, 32 endgroups, 31441 g mol^{-1}).

Peracetylated dimannose functionalized G(4)–PAMAM 8. A solution of **6** (35 mg, 46 μmol) in 1 mL DMSO was added to G(4)–PAMAM (6.3 mg, 0.47 μmol) and the solution was stirred for 48 h. Dialysis against DMSO ($\text{MWCO } 3500 \text{ g mol}^{-1}$) and lyophilization afforded 20 mg of pale yellow oily solid **8** (85% yield). $^1\text{H NMR}$ (500 MHz, CD_3SOCD_3) δ 7.93 (bs, 1H, amide NH), 7.72 (bs, 1H, amide NH), 7.44 (bs, 2H, $\text{CH}_2\text{NHC}(\text{S})\text{NHCH}_2$), 5.05–5.20 (m, 7H), 4.98 (bs, 1H), 3.99–4.09 (m, 7H), 3.88–3.89 (m, 1H), 3.74–3.79 (m, 2H), 3.56–3.63 (m, 5H), 3.48 (bs, 5H), 3.39 (m, 2H), 3.37 (s, 3H), 3.14 (bs, 3H), 3.05 (bs, 2H), 2.96 (s, 1H), 2.56–2.70 (m, 4H), 2.47 (s, 5H), 2.33–2.43 (m, 3H), 2.11–2.27 (bs, 5H), 2.07 (s, 4H), 2.00 (s, 4H), 1.98 (s, 8H), 1.95 (s, 8H), 1.92 (s, 4H) ppm; $^{13}\text{C NMR}$ (125 MHz, 1 CH_3CO overlapped) δ 172.2, 171.7, 170.5, 170.4, 170.2, 170.0, 169.9, 169.9, 169.7, 98.5, 97.9, 76.3, 69.9, 69.5, 69.2, 69.0, 68.9,

68.5, 68.3, 67.4, 67.2, 66.0, 62.5, 62.0, 50.0, 45.5, 43.7, 42.6, 38.6, 37.3, 33.7, 21.0, 21.0, 20.9, 20.8, 20.7 ppm; MALDI-TOF MS (pos) 50,400 g mol⁻¹ (theoretical MS C₂₆₀₈H₄₀₀₄N₃₁₄O₁₃₄₀S₆₄, 64 endgroups, 63250 g mol⁻¹).

Dimannose functionalized G(3)-PAMAM 9. Methanolic NaOMe (0.31 M, 93 μ L) was added to a suspension of **7** (30 mg, includes some DMSO) in MeOH : H₂O (1 : 1, 3 mL) and stirred until all the solid dissolved (*ca.* 12 h). The solution was neutralized with Amberlite IR-120 (acidic), dialyzed against water (MWCO 3500 g mol⁻¹), and filtered (Acrodisc 13 mm inline syringe with 0.2 μ m membrane). Lyophilization afforded 9.5 mg of **9** as a pale tan oily solid (*ca.* 35% yield). ¹H NMR (500 MHz, CD₃SOCD₃) δ 5.00 (s, 1H), 4.91 (s, 1H), 3.95 (s, 1H), 3.86 (s, 1H), 3.71–3.81 (m, 5H), 3.50–3.65 (m, 14H), 3.26, (bs, 5H), 2.52–3.00 (m, 6H), 2.39 (bs, 4H) ppm; ¹³C NMR (125 MHz, CD₃SOCD₃, not observed/overlapped: amide CO, CS, 2 CH₂N) δ 102.3, 98.4, 78.7, 73.3, 72.8, 70.4, 70.3, 70.0, 69.5, 68.9, 67.0, 67.0, 66.6, 61.2, 61.0, 51.7, 49.4, 43.2, 36.4, 31.8 ppm.

Dimannose functionalized G(4)-PAMAM 10. Methanolic NaOMe (0.31 M, 93 μ L) was added to a suspension of **8** (20 mg) in MeOH : H₂O (1 : 1, 3 mL) and stirred until all the solid dissolved (*ca.* 12 h). The solution was neutralized with Amberlite IR-120 (acidic), dialyzed against water (MWCO 3500 g/mol), and filtered (Acrodisc 13 mm inline syringe with 0.2 μ m membrane). Lyophilization afforded 6.8 mg of **10** as a pale tan oily solid (34% yield). ¹H NMR (500 MHz, CD₃SOCD₃) δ 5.04, (s, 1H), 4.95 (s, 1H), 3.99 (s, 1H), 3.90 (s, 1H), 3.75–3.85 (m, 6H), 3.54–3.69 (m, 15H), 3.30 (bs, 5H), 2.60–3.10 (m, 7H), 2.46 (bs, 4H) ppm; ¹³C NMR (125 MHz, CD₃SOCD₃, not observed/overlapped: amide CO, 5 CH₂N) δ 173.9, 102.3, 98.4, 78.7, 73.3, 72.9, 70.4, 70.3, 70.0, 69.5, 68.9, 67.0, 67.0, 66.6, 61.2, 61.0, 49.5, 31.5 ppm.

MALDI

Matrix assisted laser desorption ionization (MALDI) mass spectra were acquired using a Bruker Biflex-III time-of-flight mass spectrometer. Spectra of dendrimers were obtained using a *trans*-3-indoleacrylic acid matrix with a matrix : analyte ratio of 3000 : 1 or 1000 : 1. Horse heart myoglobin (MW 16952 g mol⁻¹), bovine serum albumin (MW 66431 g mol⁻¹), Bradykinin (MW 1061 g mol⁻¹), Cytochrome C (MW 12361 g mol⁻¹), and Trypsinogen (MW 23982 g mol⁻¹) were used as external standards. An aliquot corresponding to 12–15 pmol of the analyte was deposited on the laser target. Positive ion mass spectra were acquired in linear mode, and the ions were generated by using a nitrogen laser (337 nm) pulsed at 3 Hz with a pulse width of 3 ns. Ions were accelerated at 19–20000 V and amplified using a discrete dynode multiplier. Spectra (100 to 200) were summed into a LeCroy LSA1000 high speed signal digitizer. All data processing was performed using Bruker XMass/XTOF V 5.0.2. Molecular mass data and polydispersities of the broad peaks were calculated by using the Polymer Module included in the software package. The peaks were analyzed using the *continuous* mode. Delta values were set at minimum levels.

Precipitation assay

CV-N was prepared as described previously. All reactions were carried out in 110 μ L of 20 mM sodium phosphate buffer, 0.02% NaN₃, pH 6.0, in 1.5 mL microcentrifuge tubes. In different series the protein concentration varied (20–50 μ M) but was constant throughout a single series. Increasing amounts of dendrimer were added, mixed and incubated at ambient temperature for 1 h. After centrifugation (20 min) the supernatants were transferred to fresh tubes and their UV/Vis absorbance spectra were recorded. Absorbance values at 280 nm are plotted in Fig. 2. In order to test for reversible binding, the pellets were washed with 100 μ L of ice-cold buffer and dissolved in

100 μ L of 40 μ M dimannoside. Dimannose dissolved the pellet, while similar experiments with methyl mannose did not. The precipitation assay is a modification of the protocol described in reference 17. PAMAMs functionalized with **5** rather than with **6** do not cause CV-N or Con A to precipitate. Even when **5** was used at 50-fold higher concentration than **6**, no CV-N precipitation occurred.

Modelling

The maximum number of Con A lectins that can sterically fit around mannose-functionalized dendrimers of different sizes was determined using computer simulations as reported previously.^{9a} To determine how many CV-N proteins can sterically fit around the dendrimers, physical models of the appropriate sizes (spheres for dendrimers and ellipsoids for proteins) were constructed as scaled models from clay (1 Å = 1 mm). The ellipsoids were then secured to the sphere, and the maximum number that would fit was determined. As a check, similar clay models for the Con A-dendrimer systems were constructed, and the computed values were found to be in agreement with those obtained from physical models. Con A can be approximated by a sphere, which facilitates computer simulation, since modelling of spheres on spheres is a readily solvable problem.^{9a,19} Because CV-N is ellipsoidal rather than spherical, computer simulation of the CV-N-dendrimer interaction is a formidable task.

Acknowledgements

This work was supported in part by NIH RO1 GM62444 (MJC), in part by the Intramural AIDS Targeted Antiviral Program of the Office of the Director of the National Institutes of Health (AMG), in part by NSF REU and the MSU Beckman Scholars Program (SLM), and in part by the MSU BRIN (INBRE) (GCS). We thank Dr Scott Busse for help with NMR.

References

- 1 H. Geyer, C. Holschback, G. Hunsmann and J. Schneider, *J. Biol. Chem.*, 1988, **263**, 11760–11767.
- 2 J. Yeh, J. R. Seals, C. J. Murphy, J. van Halbeek and R. D. Cummings, *Biochemistry*, 1993, **32**, 11087–11099.
- 3 (a) M. R. Boyd, K. R. Gustafson, J. B. McMahon, R. H. Shoemaker, B. R. O'Keefe, T. Mori, R. J. Gulakowski, L. Wu, M. I. Rivera and C. M. Laurencot, *Antimicrob. Agents Chemother.*, 1997, **41**, 1521–1530; (b) B. R. O'Keefe, S. R. Shenoy, D. Xie, W. Zhang, J. Muschik, M. J. Currens, I. Chaiken and M. R. Boyd, *Mol. Pharmacol.*, 2000, **58**, 982–992; (c) D. S. Chan and P. Kim, *Cell*, 1998, **93**, 681–684.
- 4 (a) C. A. Bewley, K. R. Gustafson, M. R. Boyd, D. G. Covell, A. Bax, G. M. Clore and A. M. Gronenborn, *Nat. Struct. Mol. Biol.*, 1998, **5**, 571–578; (b) F. Yang, C. A. Bewley, J. M. Louis, K. R. Gustafson, M. R. Boyd, A. M. Gronenborn, G. M. Clore and A. Wlodawer, *J. Mol. Biol.*, 1999, **288**, 403–412; (c) L. G. Barrientos, J. M. Louis, D. M. Ratner, P. H. Seeberger and A. M. Gronenborn, *J. Mol. Biol.*, 2003, **325**, 211–223; (d) I. Botos, B. R. O'Keefe, S. R. Shenoy, L. K. Cartner, D. M. Ratner, P. H. Seeberger, M. R. Boyd and A. Wlodawer, *J. Biol. Chem.*, 2002, **277**, 34336–34342.
- 5 S. R. Shenoy, L. G. Barrientos, D. M. Ratner, B. R. O'Keefe, P. H. Seeberger, A. M. Gronenborn and M. R. Boyd, *Chem. Biol.*, 2002, **9**, 1109–1118.
- 6 For leading references on multivalency, see: (a) M. Mammen, S.-K. Choi and G. M. Whitesides, *Angew. Chem., Int. Ed.*, 1998, **37**, 2754–2794; (b) R. T. Lee and Y. C. Lee, *Glycoconjugate J.*, 2000, **17**, 543–551.
- 7 For leading references on protein-carbohydrate interactions, see: (a) H. Lis and N. Sharon, *Chem. Rev.*, 1998, **98**, 637–674; (b) N. V. Bovin and H.-J. Gabius, *Chem. Soc. Rev.*, 1995, **24**, 413–421; (c) N. Sharon and H. Lis, *Sci. Am.*, 1993, 82–89; (d) Y. C. Lee and R. T. Lee, *Acc. Chem. Res.*, 1995, **28**, 321–327; (e) R. A. Dwek, *Chem. Rev.*, 1996, **96**, 683–720; (f) H. J. Gabius, *Eur. J. Biochem.*, 1997, **243**, 543–576.
- 8 For some examples, see: linear polymer: (a) Z. Yang, E. B. Puffer, J. K. Pontrello and L. Kiessling, *Carbohydrate Res.*, 2002, **337**, 1605–1613; (b) L. L. Kiessling, in *Recent Trends in Molecular Recognition*, ed. F. Diederich and H. Kunzer, Springer-Verlag Berlin, Heidelberg, Berlin, 1998, pp. 183–212; (c) G. B. Sigal, M. Mammen, G. Dahmann

- and G. M. Whitesides, *J. Am. Chem. Soc.*, 1996, **118**, 3789–3800; (d) N. V. Bovin, *Glycoconjugate J.*, 1998, **15**, 431–446; (e) S. Thobhani, B. Ember, A. Siriwardena and G.-J. Boons, *J. Am. Chem. Soc.*, 2003, **125**, 7154–7155; virus cages: (f) K. S. Raja, Q. Wang and M. G. Finn, *ChemBioChem*, 2003, **4**, 1348–1351; gold nanoparticles: (g) J. Rojo, V. Diaz, J. M. de la Fuente, I. Segura, A. G. Barrientos, H. H. Riese, A. Bernad and S. Penades, *ChemBioChem*, 2004, **5**, 291–297 (h) C.-C. Lin, Y.-C. Yeh, C.-Y. Yang, G.-F. Chen, Y.-C. Chen, Y.-C. Wu and C.-C. Chen, *Chem. Commun.*, 2003, 2920–2921; Cyclodextrin: (i) A. Mazzaglia, D. Forde, D. Garozzo, P. Malvagna, B. J. Ravoo and D. Darcy, *Org. Biomol. Chem.*, 2004, **2**, 957–960 (j) T. Ooya, M. Eguchi and N. Yui, *J. Am. Chem. Soc.*, 2003, **125**, 13016–13017 (k) C. O. Mellet, J. Defaye and J. M. G. Fernandez, *Chem. Eur. J.*, 2002, **8**, 1983–1990 (l) F. Ortega-Caballero, J. J. Gimenez-Martinez, L. Garcia-Fuentes, E. Ortiz-Salmeron, F. Santoyo-Gonzalez and A. Vargas-Berenguel, *J. Org. Chem.*, 2001, **66**, 7786–6695 (m) S. Andre, H. Kaltner, T. Furuike, S.-I. Nishimura and H.-J. Gabius, *Bioconj. Chem.*, 2004, **15**, 87–98 (n) A. Nelson, J. M. Belitsky, S. Vidal, C. S. Joiner, L. G. Baum and J. F. Stoddart, *J. Am. Chem. Soc.*, 2004, **126**, 11914–11922.
- 9 (a) E. K. Woller, E. D. Walter, J. R. Morgan, D. J. Singel and M. J. Cloninger, *J. Am. Chem. Soc.*, 2003, **125**, 8820–8826; (b) E. K. Woller and M. J. Cloninger, *Org. Lett.*, 2002, **4**, 7–10; (c) E. K. Woller and M. J. Cloninger, *Biomacromolecules*, 2001, **2**, 1052–1054; (d) L. E. Samuelson, K. B. Sebby, E. D. Walter, D. J. Singel and M. J. Cloninger, *Org. Biomol. Chem.*, 2004, **2**, 3075–3079.
- 10 (a) R. Roy, *Trends Glycosci. Glycotechnol.*, 2003, **15**, 291–310; (b) R. J. Pieters, *Trends Glycosci. Glycotechnol.*, 2004, **16**, 243–254; (c) J. M. Benito, M. Gomez-Garcia, C. Ortiz Mellet, I. Baussanne, J. Defaye and J. M. Garcia Fernandez, *J. Am. Chem. Soc.*, 2004, **126**, 10355–10363; (d) S. A. Kalovidouris, O. Blixt, A. Nelson, S. Vidal, W. B. Turnbull, J. C. Paulson and J. F. Stoddart, *J. Org. Chem.*, 2003, **68**, 8485–8493; (e) I. Vrasidas, P. Valentini, C. Bock, M. Lensch, H. Kaltner, R. M. J. Liskamp, H.-J. Gabius and R. J. Pieters, *Org. Biomol. Chem.*, 2003, **1**, 803–810; (f) D. Page and R. Roy, *Bioconj. Chem.*, 1997, **8**, 714–723; (g) W. Hayes, H. M. I. Osborn, S. D. Osborne, R. A. Rastall and B. Romagnoli, *Tetrahedron*, 2003, **59**, 7983–7996; (h) S. M. Dimick, S. C. Powell, S. A. McMahon, D. M. Moothoo, J. H. Naismith and E. J. Toone, *J. Am. Chem. Soc.*, 1999, **121**, 10286–10296.
- 11 G. R. Newkome, C. N. Moorefield, F. Vögtle, in *Dendrimers and Dendrons: Concepts, Syntheses, Applications*; Wiley-VCH: Weinheim, 2001.
- 12 M. J. Cloninger, *Curr. Opin. Chem. Biol.*, 2002, **6**, 742–748.
- 13 T. Ren and D. Liu, *Tetrahedron Lett.*, 1999, **40**, 7621–7625.
- 14 J. O. Deffarari, E. G. Gros and I. O. Mastronardi, *Carbohydr. Res.*, 1967, **4**, 432–434.
- 15 M. Upreti, D. Ruhel and R. A. Vishwakarma, *Tetrahedron*, 2000, **56**, 6577–6584.
- 16 (a) Tomalia *et al.* have reported that the average molecular weights of PAMAM dendrimers are smaller than the theoretical weights; our MALDI results are consistent with Tomalia's electrospray results: L. P. Tolic, G. A. Anderson, R. D. Smith, H. M. Brothers, R. Spindler and D. A. Tomalia, *Int. J. Mass Spectrom. Ion Processes*, 1997, **165/166**, 405–418; (b) incomplete Michael addition or retro-Michael reaction is the most significant cause of dendrimer defects: J. Peterson, V. Allikmaa, J. Subbi, T. Pehk and M. Lopp, *Eur. Polym. J.*, 2003, **39**, 33–42; (c) for a more in-depth discussion of MALDI-TOF MS characterization of mannose functionalized dendrimers, see reference 9c.
- 17 K. M. Islam, D. K. Mandal and C. F. Brewer, *Carbohydr. Res.*, 1991, **213**, 69–77.
- 18 D. K. Mandal, N. Kishore and C. F. Brewer, *Biochemistry*, 1994, **33**, 1149–1156.
- 19 The work of N. J. A. Sloane; for more information about spherical packings, see: <http://www.research.att.com/~njas/>.